Proceedings of the
Annual Stability Conference
Structural Stability Research Council
St. Louis, Missouri, April 2-5, 2019

Stability of aboveground open-top storage tanks subjected to wind loading: static and dynamic analyses

Yen-Chen Chiang[1], William B. Rich[2], Sukru Guzey[3]

Abstract
Boundary layer wind tunnel tests have shown that when open-top storage tanks are subjected to wind loading, an internal inward pressure is generated, which is a phenomenon not observed when close-top tanks are examined. This internal pressure is accounted for in both European and Australian/New Zealand design documents, but may not be sufficiently addressed in North American design documents such as ASCE-7, API 650 and AWWA D-100. To investigate the adequacy of these documents, above ground open-top steel tanks with a wide range of height to diameter ratios (H/D), were examined. The tanks were subjected to multiple finite element analyses including a linear bifurcation analysis, a static geometric nonlinear analysis with imperfections, and an explicit dynamic analysis. It was found that the internal pressure significantly affected the buckling capacity of a tank, and revisions of the structural stability and wind girder design guidelines were suggested for North American design documents. Resonance was not observed in the analyses when dynamic effects were considered, and the differences between the result of the dynamic and static analyses for broad tanks ($H/D < 1.0$) were minor. Therefore, it was concluded that a static analysis is adequate for a practical tank design.

1. Introduction

Aboveground steel storage tanks are widely employed in various industries for storing liquids such as water, chemicals, oil, etc. (DiGrado and Thorp 1995; Myers 1997). To make these tanks cost-efficient, the shells of such tanks are usually made as thin as possible (Azzuni and Guzey 2015; Zick and McGrath 1968). As a consequence of this thin geometry, tanks are prone to buckling induced by various events, such as seismic excitation, internal vacuum, and wind gusts (Godoy 2016).

Ground motions can be critical when tanks are full, and thus, this problem has been extensively studied (Haroun and Housner 1981; Housner 1963; Jacobsen 1949; Spritzer and Guzey 2017; Veletsos 1984). Internal vacuums (which are usually caused by operational errors) (Godoy 2016) are another critical event which has garnered much research (Chen et al. 2012; von Mises 1931).

[1] Graduate research assistant, Lyles School of Civil Engineering, Purdue University, <chiang45@purdue.edu>
[2] Graduate research assistant, Lyles School of Civil Engineering, Purdue University, <rich31@purdue.edu>
[3] Assistant professor, Lyles School of Civil Engineering, Purdue University, <guzey@purdue.edu>

When tanks are empty, however, wind gusts are the primary factor affecting the stability of the tanks.

For an open-top tank, if there is no constraint along the top edge, the general buckling, in which the top edge of a tank cannot maintain its circular profile may occur. To avoid such an unfavorable phenomenon, top wind girders are introduced to open-top tanks. The proper method for sizing wind girders has also attracted researchers' attention (AWWA 1935; Azzuni and Guzey 2018; Bu and Qian 2016; McGrath 1963).

Boundary layer wind tunnel tests (BLWT) have been the major method utilized when examining how wind gusts interact with tanks. Based on the results of the BLWT conducted by researchers (Macdonald et al. 1988; Sabransky and Melbourne 1987; Uematsu et al. 2014), it was determined that for an open-top tank, a significant internal inward pressure is created by a wind gust. This behavior is addressed in design documents such as EN1993-4-1 (European Committee for Standardization 2007) and AS/NZS 1170.2:2011 (Joint Standards Australia/Standard New Zealand Standard 2011), but is not explicitly considered in North American design documents such as API 650 (API 2013), AWWA D100-11 (AWWA 2011), or ASCE-7 (American Society of Civil Engineers 2016).

Using the wind pressure distributions obtained from BLWT, the buckling behavior of tanks has been extensively studied in the past few decades using the finite element method (FEM). To verify the stability of tanks under wind loading, most researchers chose to conduct static analyses because dynamic effects were considered negligible (Sosa and Godoy 2005; Uematsu et al. 2015). Common static analysis methods include the linear bifurcation analysis (LBA) and the static geometric nonlinear analysis with imperfections (GNIA). Using these and other approaches, the buckling behavior of tanks under wind loading has been investigated by many researchers (Greiner and Derler 1995; Shokrzadeh and Sohrabi 2016; Sun et al. 2018; Zhao and Lin 2014).

In the design procedure specified in API 650, the internal inward pressure is not accounted for. Therefore, the stability of open-top tanks under wind loading is questionable. Additionally, the circumferential pressure profile used for design in API 650 and ASCE-7 varies drastically from the BLWT results. To the authors' best knowledge, no study has been dedicated to analyzing the buckling capacity of open-top API 650 tanks subjected to wind loading that follows wind profiles whose circumferential distribution were originated from BLWT. Thus, this study aims to verify whether tanks designed in conformance with current design provision are able to withstand wind gusts if the wind pressure profile applied is more realistic.

Three tanks with height to diameter ratios of 2.0, 1.0, and 0.2 were examined. Analyses using a finite element program were conducted. An LBA, a static GNIA, and an explicit dynamic analysis were conducted. The tanks' buckling capacities obtained through these analyses were compared to the design wind pressure, and the effects of the aspect ratio (H/D, where H is the height of a tank and D is the diameter of a tank) were discussed. The dynamic analysis portion was an extension of the work done by Sosa and Godoy (Sosa and Godoy 2005). Though Sosa and Godoy concluded that dynamic effects were subtle, only tanks with an aspect ratio of 0.4 and a conical roof were adopted in their study. In the present study, open-top tanks with a wider spectrum of aspect ratios were studied to investigate how resonance may affect the buckling capacity of tanks.

2. Methodology

2.1. Tank Design

Three empty aboveground open-top tanks were examined in this study. All three tanks were composed of five 2.44 m high shell courses with a total height of 12.2 m. The diameter of these three tanks were 6.10 m (Tank A), 12.2 m (Tank B), and 61.0 m (Tank C). The shell thicknesses of Tanks A and B were designed using the 1-foot method specified in API 650, while Tank C was designed following the variable-design-point method in API 650. The material selected for the tanks was mild carbon steel with a Young's modulus (E) of 200 GPa, a Poisson's ratio (v) of 0.3, a mass density of 7900 kg/m^3, and an allowable stress of 159 MPa. The specific gravity of the liquid stored in the tanks was 1.0, and the corrosion allowance was zero. The geometries and shell thicknesses for all three tanks can be found in Table 1.

Table 1: Tank geometries and shell thicknesses of the modeled tanks.

Tank name	Height (m)	Diameter (m)	Aspect ratio (H/D)	Shell thickness (mm)				
				1	2	3	4	5
A	12.2	6.10	2.0	6.0	5.0	5.0	5.0	5.0
B	12.2	12.2	1.0	6.0	5.0	5.0	5.0	5.0
C	12.2	61.0	0.2	22	17	12	8.0	8.0

In the present study, top wind girders were included for all three tanks, and the wind girders were sized assuming a design wind speed of 145 km/hr. The dimensions of the top wind girders are compiled in Table 2. Details for the top wind girders can be found in API 650 (API 2013) Paragraph 5.9.6.3. The wind girder on Tank B is an angle profile with the long leg placed horizontally.

Table 2: Dimensions of installed top wind girders.

Tank name	Detail type	Size (mm)	Distance from top edge (cm)	Section modulus (cm^3)
A	b	L65x65x6	2.5	27
B	c	L100×75×8	8.0	67
C	e	b = 800	13	1600

2.2. Static analysis

For a practical design, static analyses are usually adequate and are widely performed. An LBA and a static GNIA were adopted in this study.

An LBA is a suitable type of analysis for a preliminary design due to its simplicity and computational efficiency. By conducting an LBA, the upper bound of the buckling capacity (eigenvalue) and the buckling mode shape (eigenvector) of a tank, assuming elastic and geometrically perfect conditions, can be obtained.

It is well-known that thin cylindrical shells are prone to buckling, and that the buckling behavior is heavily dependent on localized imperfection. To take this factor into consideration, an artificial imperfection, such as an eigen-affine imperfection, is widely adopted. When imperfections are

accounted for, a static GNIA predicts the behavior of a tank less conservatively than an LBA. During an analysis, the nodes of a geometrically perfect tank will be distributed according to the first buckling mode shape. Then, the external load (e.g. wind loading) will be applied to the tank incrementally to capture the geometric nonlinearity using the arc-length algorithm (Riks method). The magnitudes of the imperfections adopted in this study were 0.01*t*, 0.1*t*, 0.5*t*, and 1*t*, where *t* is the tank's thinnest shell thickness.

In most of the analyses, the circumferential wind distribution applied to the tanks followed the wind profile specified in EN-1993-4-1 (European Committee for Standardization 2007), and can be expressed as in Eq. 1.

$$\begin{aligned} C_{pe}(\theta) = &-0.54 + 0.16(D/H) + [0.28 + 0.04(D/H)]cos(\theta) \\ &+[1.04 - 0.20(D/H)]cos(2\theta) + [0.36 - 0.05(D/H)]\,cos(3\theta) \\ &-[0.14 - 0.05(D/H)]\,cos(4\theta) \end{aligned} \quad (1)$$

In Eq. 1, $C_{pe}(\theta)$ is the normalized external circumferential pressure distribution (positive indicates a pressure toward the surface), and θ is the circumferential position where the wind pressure is being considered. The $C_{pe}(\theta)$ distribution for all three tanks are shown in Figure 1.

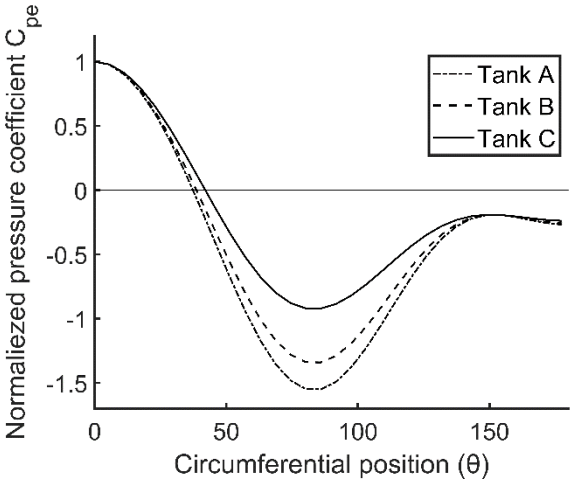

Figure 1: The normalized external circumferential pressure distribution specified in EN1993-4-1 for Tanks A, B and C.

EN1993-4-1 also requires that an internal inward pressure, C_{pi}, be applied to open-top tanks. The internal pressure is a constant value of -0.6 regardless of circumferential position and tank geometry. The pressure applied to the tank shells is the product of *P* and C_p, where *P* is the product of the velocity pressure and the gust factor, and C_p is the difference between C_{pe} and C_{pi}. In contrast to the wind profile specified in API 650 (API 2013) and ASCE-7 (American Society of Civil Engineers 2016), which dictate that the wind should be uniformly distributed on the projected area of a tank with a magnitude of 0.63*P*, the wind profile specified in EN1993-4-1 is more similar to the distributions obtained through BLWT, and thus, more realistic. Moreover, the internal inward pressure for open-top tanks considered in API 650 is much smaller than the internal pressure required by EN-1993-4-1. In accordance with API 650, the internal pressure (C_{pi}) is approximately 14% of the external pressure at the stagnation point ($C_{pe}(0°)$) (McGrath 1963),

while it is 60% of the external pressure at the stagnation point in EN 1993-4-1. Note that the wind pressure was assumed to be constant along the tank height, since the tanks were relatively short and this assumption is similar to vertical wind profile specified in ASCE-7.

2.3. Dynamic analysis

By conducting dynamic analyses, the possibility of a tank experiencing resonance can be examined. Since an explicit dynamic analysis assumes that the mass and the stiffness matrix are known, and that the displacement/velocity are directly calculated from the previous time increment, the analysis is computationally efficient. Note that geometric nonlinearity was accounted for in the dynamic analyses, but damping was not considered in this study.

To investigate whether a geometrically perfect tank would face resonance, the natural vibration frequencies are first determined using FEM. By solving for the natural vibration frequencies, the first natural vibration frequency of each system, which usually has the largest modal participation factor, can be obtained. The wind gusts are assumed to be vibrating at the natural vibration frequencies. A schematic of the wind action model adopted in this study is shown in Figure 2.

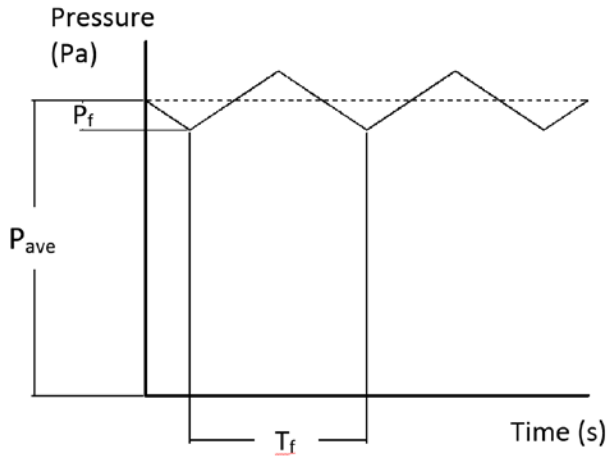

Figure 2: Illustration of the wind action model utilized during the dynamic analyses.

In Figure 2, P_{ave} represents the average wind pressure, with a magnitude equivalent to P, P_f represents the magnitude of a minor fluctuation, and T_f represents the fluctuation period. In this study, P_f was selected to be 0.1 times the magnitude of $P_{ave,}$ and a wind gust duration of nine seconds was selected.

Compared to the other types of analyses, a dynamic analysis with a geometric imperfection yields the lowest buckling capacity, and thus such an analysis should be carried out. Since taller tanks are less prone to eigen-affine imperfections (Godoy and Flores 2002), imperfections were only introduced to broad tanks (Tank C) during the dynamic analyses.

2.4. Finite element models

Finite element models for all three tanks were constructed in ABAQUS ver. 2018 (ABAQUS 2018). The element type selected was S4R, which is a reduced integration, 4-node, quadrilateral shell element with large strain formulation. To scale the mesh size of the models, a mesh scaling index, $\beta\sqrt{Rt}$, was used. Here R is the radius of a tank, and β is a scaling factor. For the static

analyses, the mesh scaling factor β was 0.5 (fine mesh), and for the dynamic analysis, β was 1.76 (coarse mesh). The only exception was Tank A, for which the fine mesh was adopted for both analysis types. The reasons for this exception will be addressed later. The mesh sizes are presented in Table 3.

Table 3: Mesh sizes for the modeled tanks.

	Mesh size (cm)	
Tank name	Static analysis	Dynamic analysis
A	6.1	6.1
B	8.7	31
C	25	85

Using Tank B as an example, the elements utilized for the static analyses model were squares with approximate dimensions of 8.7 cm × 8.7 cm, while the elements for dynamic analysis models were squares with approximate dimensions of 31 cm × 31 cm. The boundary conditions for all the models consisted of fixed bottom edges and free top edges. Note that to properly capture the behavior of the wind girders, at least four elements were assigned along the depth of the wind girders. Models of Tank B for both the static and the dynamic analyses are shown in Figure 3.

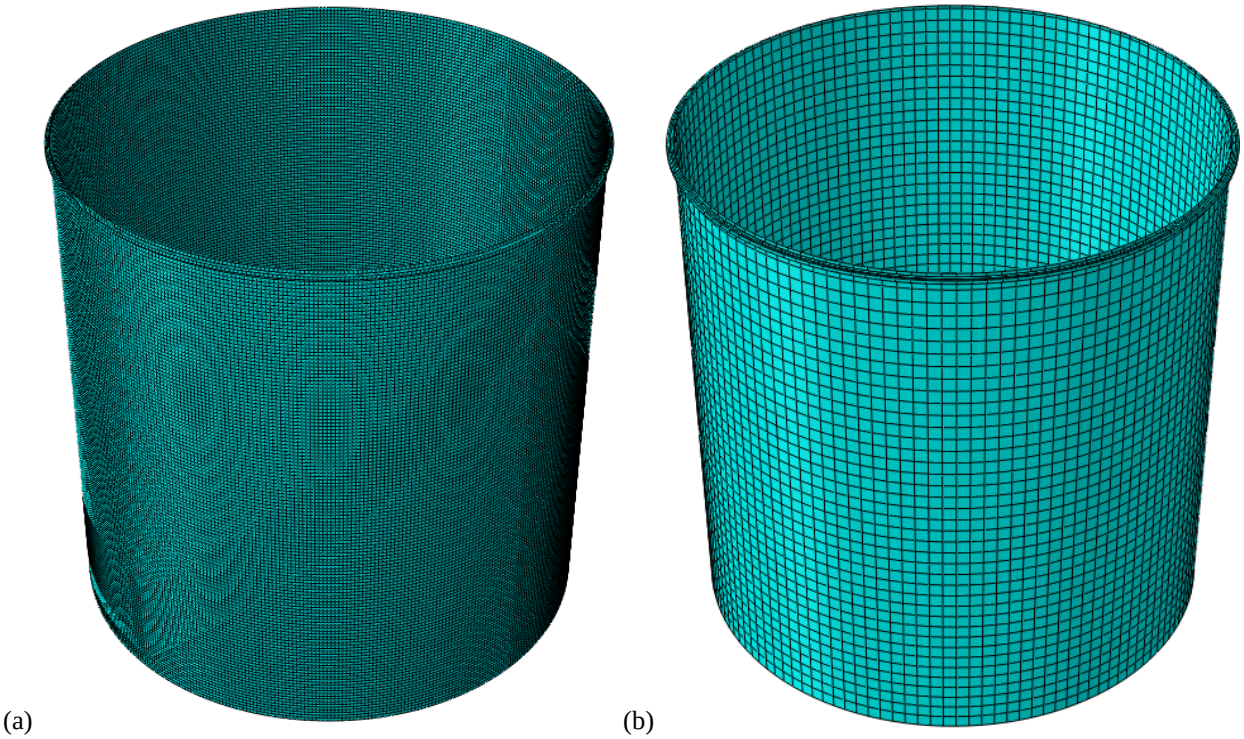

(a) (b)

Figure 3: Tank B with (a) 64380 S4R elements (fine mesh) and (b) 5980 S4R elements (coarse mesh).

3. Results and Discussion

3.1. Static analysis

The buckling capacities obtained through the LBA with the fine mesh were 5,691 Pa, 1,828 Pa, and 877.3 Pa for Tanks A, B, and C, respectively. Note that the design wind pressure corresponding to a design wind speed of 145 km/hr in API 650 is 838.8 Pa. The LBA buckling capacity of Tank C is barely higher than the design pressure, indicating that buckling capacity of Tank C is inadequate. It should be noted the unstiffened height of Tank C is only slightly larger than the maximum allowable unstiffened height. However, this should not have a drastic impact on the reslt of analysis. If the wind pressure applied was in accordance with the API 650 wind profile, the LBA buckling capacity would be 2048 Pa. The difference between the buckling capacities obtained using the different wind profiles is the result of the internal pressure in API 650 being much lower, and the circumferential distribution varies greatly from the experimental results of MacDonald et al (Macdonald et al. 1988). It seems that the design guideline of wind girder may need to be improved to provide adequate buckling capacity.

Using the first eigenmode shapes obtained from the LBA employing the EN1993-4-1 wind profile, static GNIA were conducted for various imperfection amplitudes. The results of the static GNIA are complied in Figure 4. In Figure 4, the *x*-axis represents the magnitude of the displacement history of the node at which the onset of the buckling occurred normalized with respect to *t*, and the *y*-axis represents the applied pressure (*P*) normalized with the design pressure of 838.8 Pa. It can be observed that Tank A has at least five times the buckling capacity compared to the design pressure, and Tank B buckles at a pressure that is 1.5 times higher than the design pressure even when an imperfection amplitude of 1.0*t* was applied. However, Tank C has a relatively low buckling capacity, which results in the buckling capacity being less than the design pressure even at mild imperfection amplitudes such as 0.1*t*. In this scenario, Tank C is vulnerable to buckling.
The high buckling capacities of Tanks A and B might be a result of the smaller diameter to shell thickness ratios compare to that of Tank C. Although the design procedures of all three tanks were similar, the shell thicknesses for all Tanks A and B courses were governed by the minimum shell thickness specified in API 650. In other words, compared to Tank C, whose shell was designed to withstand the hydrostatic pressure created by the liquid stored in it, the shells of Tanks A and B can carry a larger external load. The *D/t* ratio of the tanks were 1,220, 2,440, and 7,620 for Tanks A, B, and C, respectively. There is a trend that when the diameter of a tank increases, the *D/t* ratio increases. The *D/t* ratio of Tank A is around one-sixth the *D/t* ratio of Tank C, resulting in a huge difference in buckling capacity.

The sensitivity of a tank to imperfections is also heavily dependent on the tank's height to diameter aspect ratio. In Figure 4, it can be observed that the lower the aspect ratio of a tank, the higher the sensitivity to eigen-affine imperfection. This result aligned with the results reported by other researchers (Godoy and Flores 2002; Greiner and Derler 1995).

3.2. Dynamic analysis

To investigate the possibility of resonance affecting the stability of a tank, natural vibration frequency analyses and dynamic analyses were conducted. The first natural vibration frequencies were 8.11 Hz, 5.75 Hz, and 4.92 Hz, for Tanks A, B, and C, respectively. The reciprocals of these

frequencies were used as T_f (see Figure 2). The buckling capacities were determined using a criterion proposed by Budiansky and Roth (Budiansky and Roth 1962).

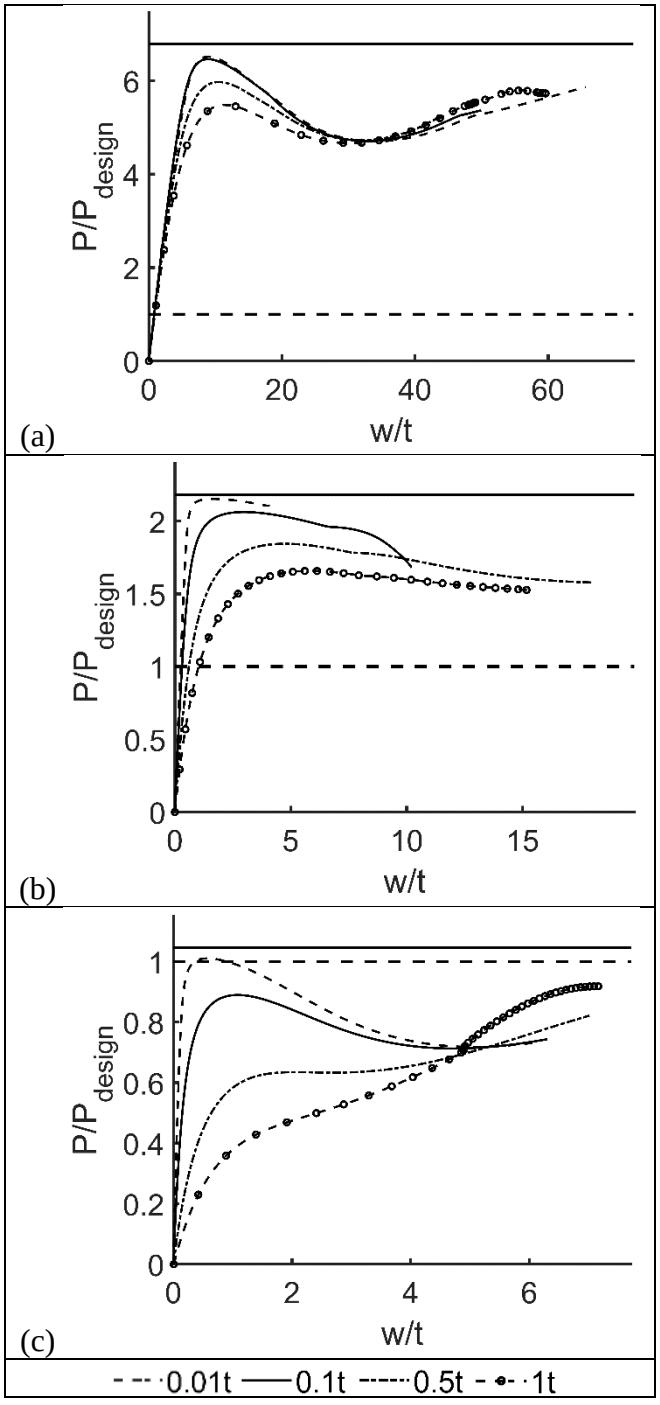

Figure 4: The static GNIA results for all three tanks using the EN1993-4-1 wind profile. A horizontal solid line represents the LBA buckling capacity, and a horizontal dotted line represents the design wind pressure. (a) Tank A, (b) Tank B, (c) Tank C.

The dynamic buckling capacities obtained for Tanks A, B and C were 4,000 Pa, 1,650 Pa, and 1,000 Pa, respectively. Note that the dynamic analyses of Tanks B and C were conducted using a coarser mesh than during the static analyses, and the buckling capacities obtained through the LBA using this mesh size were 1,624 Pa and 1,010 Pa for Tanks B and C, respectively. Comparing the dynamic buckling capacities and the LBA buckling capacities of Tanks B and C, results in only minor difference. However, for Tank A, there is a 30% difference, which is significant. To study this behavior carefully, a fine mesh was adopted even during the dynamic analyses.

This difference is a result of the different buckling shapes obtained from the dynamic analysis and the LBA. The deflected shape of Tank A obtained from the dynamic analysis and the LBA can be found in Figure 5, and it can be observed that the deflected shapes of these two analyses are remarkably different.

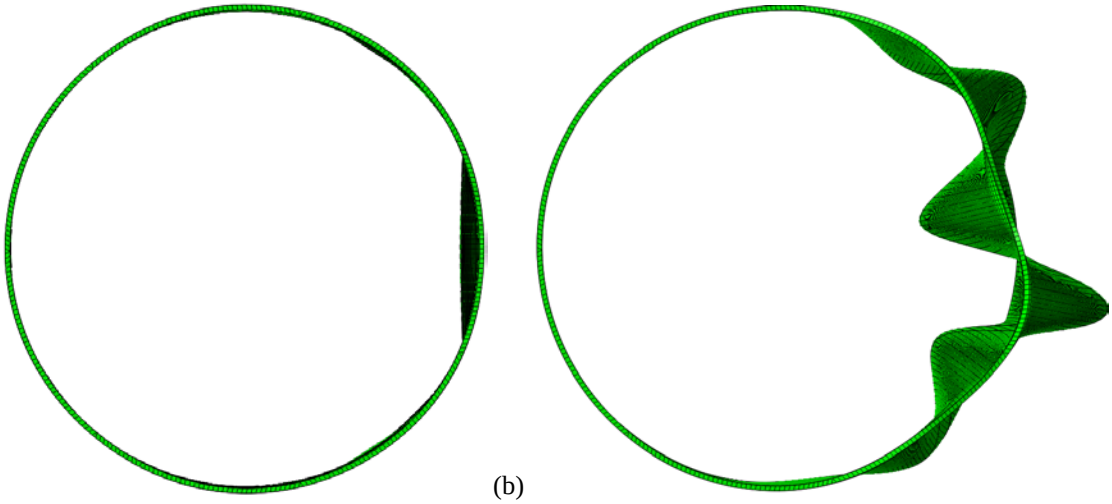

(a) (b)

Figure 5: The top view of the deflected shape of Tank A. Wind blowing from right to the left. (a) Deflected shape of Tank A when the onset of buckling occurred. Obtained using a dynamic analysis. P=4000 Pa. (b) First mode shape obtained from the LBA.

The difference occurs because the geometric nonlinearity is only considered in the dynamic analysis. Comparing the buckling capacity obtained from the dynamic analysis to the buckling capacity obtained by the static GNIA with an imperfection amplitude of 0.01t (see Figure 4) produces a smaller difference. The buckling capacity of the static GNIA was 5,235 Pa, which result in a difference of 24% between the static GNIA and the dynamic analysis. It appears that since both the static GNIA and the dynamic analysis consider geometric nonlinearity, the results have an improved agreement.

Despite the drop in buckling capacity observed during the dynamic analysis, the resulting behavior was not considered to be a resonance, because similar drops in buckling capacity were observed when wind gusts fluctuated at different frequencies. The dynamic analysis results of Tank A with different fluctuation periods are presented in Figure 6. Note that T_f was only considered up to three seconds because the wind velocity is typically recorded every three seconds (Sosa and Godoy 2005). The objective here was to investigate whether a minor fluctuation with a period less than three second would cause resonance. Since the buckling capacities obtained from the different

fluctuation periods are similar, the dynamic responses obtained from the different fluctuation periods are not considered to be resonance.

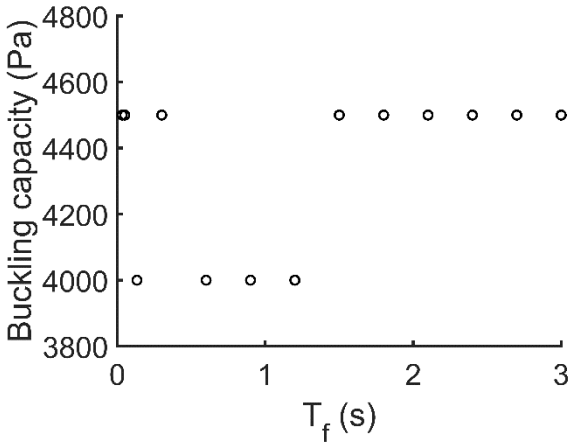

Figure 6: Dynamic analysis results of Tank A with different fluctuation periods.

To investigate the worst case scenario, dynamic analyses of Tank C with different imperfections were carried out. Note that even though dynamic effects are most prominent for Tank A, Tank A was not adopted in this section since Tank A is not sensitive to eigen-affine imperfections. The dynamic buckling capacities of Tank C were 950 Pa, 850 Pa, and 600 Pa with imperfection amplitudes of 0.01*t*, 0.1*t*, and 0.5*t*, respectively. Using the same imperfection amplitudes, the buckling capacities obtained through the static GNIA with the coarse mesh were 970 Pa, 877 Pa, and 709 Pa, respectively. Therefore, the buckling capacities obtained from the dynamic analyses and the static GNIA have a good agreement, even though there is a 15% difference bewteen the results when the imperfection amplitude was set to 0.5*t*. The buckling behavior resulting from a dynamic analysis of Tank C with a 1.0*t* amplitude imperfection cannot be well-defined. Displacement time histories of the node at which the onset of buckling occurred on Tank C are shown in Figure 7. It can be observed that there is no distinguishable difference between the time histories. Similarly, the static GNIA with an imperfection amplitude of 1.0*t* in Figure 4 does not show a distinct peak in the loading path. It can thus be stated that, for Tank C, the behaviors obtained through a dynamic analysis and a static analysis are similar.

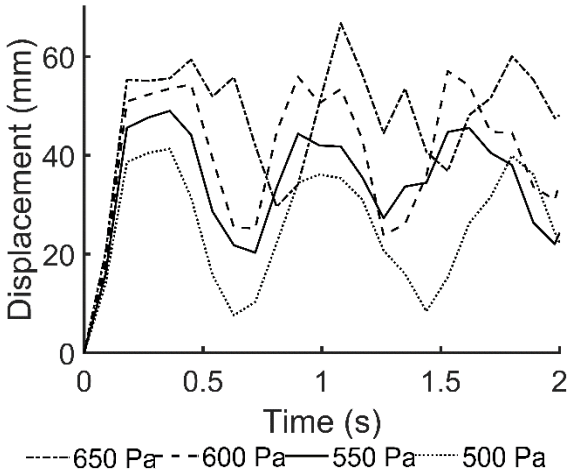

Figure 7: Displacement time histories of Tank C with an imperfection amplitude of 1.0*t* under different pressure levels.

4. Conclusions

This paper examines the buckling capacity of empty tanks under wind loading. The three analysis types adopted were an LBA, a static GNIA, and a dynamic analysis. Three tanks with aspect ratios ranging from 0.2 to 2.0 were examined. By conducting these analyses, the stability of these tanks was examined.

By conducting static analyses, it was determined that the adequacy of the buckling capacity was dependent upon the tank geometry. For Tanks A and B, the buckling capacities appears to be adequate when compared to the API 650 design pressure. However the adequacy of buckling capacity of Tank C is questionable. This is partially due to the high D/t ratio of Tank C, which results from the shell of Tank C being designed to withstand the hydrostatic pressure that would be created by the liquid stored in the tank. Additionally, the inadequacy in the buckling capacity of Tank C is also a result of the inappropriate wind pressure distribution specified in ASCE-7 and API 650. If Tank C is subjected to the wind pressure produced by the API 650 wind profile, the buckling capacity becomes adequate.

To further investigate the stability of the tanks, dynamic analyses were conducted. The first natural vibration frequencies of all three tanks were first obtained by FEM. The wind pressure was then assumed to be vibrating at these frequencies. It was found that the buckling capacities obtained through a static analysis and a dynamic analysis without imperfections do not differ from each other for Tanks B and C. For Tank A, even though the dynamic analyses resulted in a drop in buckling capacities when compared to the static analyses, the behavior observed was not considered resonance. Moreover, dynamic analyses including imperfections were also carried out using Tank C, since Tank C was most prone to eigen-affine imperfections. The buckling capacities obtained from the dynamic analyses with imperfections barely differed from the buckling capacities obtained from the static GNIA. Thus, it can be concluded that a static analysis is adequate for practical tank designs, but an appropriate safety factor should be taken into account, especially for tanks with large aspect ratios.

Acknowledgements

Research conducted by the first author was supported by the Goldberg Fellowship and Purdue University.

References

ABAQUS (2018). *ABAQUS Analysis User's Manual version 2018*, Dassault Systèmes SIMULIA, Providence, RI.

American Society of Civil Engineers (2016). *ASCE-7-16: Minimum Design Loads for Building and other Structures*, ASCE-7-16, Reston, VA.

API (2013). *Welded Tanks for Oil Storage*, American Petroleum Institue, Washington, DC. API Standard No.650.

AWWA (1935). *Standard Specifications for Elevated Steel Water Tanks, Standpipes and Reservoirs*, American Water Work Association, Denver, CO.

AWWA (2011). *Welded Carbon Steel Tanks for Water Storage*, American Water Works Association, Denver, CO AWWA standard D100-11.

Azzuni, E., Guzey, S. (2015). "Comparison of the shell design methods for cylindrical liquid storage tanks." *Engineering Structures*, Elsevier, 101, 621-630.

Azzuni, E., Guzey, S. (2018). "A perturbation approach on buckling and postbuckling of circular rings under nonuniform loads." *International Journal of Mechanical Sciences*, Elsevier, 137, 86-95.

Bu, F., Qian, C. (2016). "On the rational design of the top wind girder of large storage tanks." *Thin-Walled Structures*, Elsevier, 99, 91-96.

Budiansky, B., Roth, R. S. (1962). "Axisymmetric dynamic buckling of clamped shallow spherical shells." *NASA Collected Papers on Stability of Shell Structure*, Nasa Technical Report Sever, 597-606.

Chen, L., Rotter, J. M., Doerich-Stavridis, C. (2012). "Practical calculations for uniform external pressure buckling in cylindrical shells with stepped walls." *Thin-Walled Structrures*, Elsevier, 61, 162-168.

DiGrado, B. D., Thorp, G. A. (1995). *The aboveground steel storage tank handbook*, John Wiley & Sons Inc, Hoboken, NJ.

European Committee for Standardization (2007). *Eurocode 3: Design of Steel Structures, Part 4.1: Silos*, Standard No. EN 1993-4-1, Brussels, Belgium.

Godoy, L. A. (2016). "Buckling of vertical oil storage steel tanks: Review of static buckling studies." *Thin-Walled Structures*, Elsevier, 103, 1-21.

Godoy, L. A., Flores, F. G. (2002). "Imperfection sensitivity to elastic buckling of wind loaded open cylindrical tanks." *Structural Engineering and Mechanics*, Techno Press, 13(5), 533-542.

Greiner, R., Derler, P. (1995). "Effect of imperfections on wind-loaded cylindrical shells." *Thin-Walled Structures*, Elsevier, 23(1-4), 271-281.

Haroun, M., Housner, G. (1981). "Earthquake response of deformable liquid storage tanks." *Journal of Applied Mechanics*, The American Society of Mechnical Engineers, 48(2), 411-418.

Housner, G. W. (1963). "The dynamic behavior of water tanks." *Bulletin of the seismological society of America*, Seismology Society of America, 53(2), 381-387.

Jacobsen, L. S. (1949). "Impulsive hydrodynamics of fluid inside a cylindrical tank and of fluid surrounding a cylindrical pier." *Bulletin of the Seismological Society of America*, Seismology Society of America, 39(3), 189-204.

Joint Standards Australia/Standard New Zealand Standard (2011). *AS/NZS 1170.2: 2011 Structural design actions-Part 2: Wind actions*, Sydney, NSW, Australia.

Macdonald, P., Kwok, K., Holmes, J. (1988). "Wind loads on circular storage bins, silos and tanks: I. Point pressure measurements on isolated structures." *Journal of Wind Engineering and Industrial Aerodynamics*, Elsevier, 31(2-3), 165-187.

McGrath, R. V. "Stability of API standard 650 tank shells." *Proc., 28th Midyear meeting of the American Petroleum Institute's division of refining*, American Petroleum Institute.

Myers, P. E. (1997). *Aboveground storage tanks*, McGraw-Hill, New York, NY.

Sabransky, I., Melbourne, W. (1987). "Design pressure distribution on circular silos with conical roofs." *Journal of Wind Engineering and Industrial Aerodynamics*, Elsevier, 26(1), 65-84.

Shokrzadeh, A. R., Sohrabi, M. R. (2016). "Buckling of ground based steel tanks subjected to wind and vacuum pressures considering uniform internal and external corrosion." *Thin-Walled Structures*, Elsevier, 108, 333-350.

Sosa, E. M., Godoy, L. A. (2005). "Nonlinear dynamics of above-ground thin-walled tanks under fluctuating pressures." *Journal of sound and vibration*, Elsevier, 283(1-2), 201-215.

Spritzer, J., Guzey, S. (2017). "Nonlinear numerical evaluation of large open-top aboveground steel welded liquid storage tanks excited by seismic loads." *Thin-Walled Structures*, Elsevier, 119, 662-676.

Sun, T., Azzuni, E., Guzey, S. (2018). "Stability of Open-Topped Storage Tanks With Top Stiffener and One Intermediate Stiffener Subject to Wind Loading." *Journal of Pressure Vessel Technology*, The American Society of Mechnical Engineers, 140(1), 011204.

Uematsu, Y., Koo, C., Yasunaga, J. (2014). "Design wind force coefficients for open-topped oil storage tanks focusing on the wind-induced buckling." *Journal of Wind Engineering and Industrial Aerodynamics*, Elsevier, 130, 16-29.

Uematsu, Y., Yasunaga, J., Koo, C. (2015). "Design wind loads for open-topped storage tanks in various arrangements." *Journal of Wind Engineering and Industrial Aerodynamics*, Elsevier, 138, 77-86.

Veletsos, A. (1984). "Seismic response and design of liquid storage tanks." *Guidelines for the seismic design of oil and gas pipeline systems*, American Society of Civil Engineers, 255-370.

von Mises, R. (1931). *The critical external pressure of cylindrical tubes*, US Experimental Model Basin, Navy Yard, Washington DC.

Zhao, Y., Lin, Y. (2014). "Buckling of cylindrical open-topped steel tanks under wind load." *Thin-Walled Structures*, Elsevier, 79, 83-94.

Zick, L., McGrath, R. (1968). "Design of Large Diameter Cylindrical Shells." *Proceedings—API Division of Refining, American Petroleum Institute, New York*, 48, 1114-1140.